Supporting Information

Kinetics and Products of the Reaction of the First-Generation Isoprene Hydroxy Hydroperoxide (ISOPOOH) with OH

Jason M. St. Clair[†], *Jean C. Rivera-Rios*[‡], *John D. Crounse*[†], *Hasse C. Knap*[§], *Kelvin H. Bates#, Alex P. Teng*[†], *Solvejg Jørgensen*[§], *Henrik G. Kjaergaard*[§], *Frank N. Keutsch*[‡ψ], *Paul O. Wennberg*[†⊗]

[†]Division of Geological and Planetary Sciences, California Institute of Technology, 1200 E. California Blvd, Pasadena, CA 91125

[‡]Department of Chemistry, University of Wisconsin-Madison, 1101 University Avenue, Madison, WI 53706

ψ Paulson School of Engineering and Applied Sciences and Department of Chemistry and Chemical Biology, Harvard University, 12 Oxford Street, Cambridge MA 02138

[§]Department of Chemistry, DK-2100 Copenhagen Ø, University of Copenhagen,

Copenhagen, Denmark

#Division of Chemistry and Chemical Engineering, California Institute of Technology, 1200 E. California Blvd, Pasadena, CA 91125

⊗Division of Engineering and Applied Science, California Institute of Technology, 1200 E. California Blvd, Pasadena, CA 91125

S1.0 CIMS Sensitivities CIMS sensitivities to the oxidation products were determined in multiple ways. Hydroxyacetone and glycolaldehyde are commercially available and were quantified gravimetrically and by Fourier Transform Infrared Spectroscopy (FT-IR) for CIMS calibration.[1] Uncalibrated compounds (glycolic acid and all products identified by *m/z*) were assigned a generic CIMS sensitivity of 2.5×10^{-4} ncts /pptv, and are considered accurate to within a factor of 2. Here, normalized counts (ncts) represent the counts observed at the analyte *m/z* divided by the reagent ion counts. The reagent ion counts are the sum of the signal at *m/z* = 86 ($^{13}CF_3O^-$) and *m/z* = 104 ($^{13}CF_3O^- \bullet H_2O$), as well as *m/z* = 120 ($^{13}CF_3O^- \bullet H_2O_2$) for experiments with H_2O_2 as the OH source.

The sensitivities for ISOPOOH and IEPOX were obtained by matching the output of a box model to a laboratory isoprene + OH oxidation under low NO conditions. The sensitivity is therefore dependent on the box model chemistry, including the yield of ISOPOOH from isoprene (0.94) and the yield of IEPOX from ISOPOOH (0.8). The ISOPOOH yield used was based on a 6% yield of methyl vinyl ketone and methacrolein,[2] and the IEPOX yield used was 80%, in general agreement with the sum of the non-IEPOX products observed by the CIMS in this study. ToF-CIMS sensitivities for ISOPOOH and IEPOX were 1.6×10^{-4} ncts/pptv and 1.9×10^{-4} ncts/pptv, respectively. For the TQ-CIMS, the MSMS sensitivities were 5.1×10^{-6} ncts/pptv and 3.9×10^{-6} ncts/pptv for ISOPOOH and IEPOX, respectively. The CIMS sensitivity to ISOPOOH was also verified gravimetrically by completely evaporating a known mass of the pure compound into a known volume of dry air. For the (4,3)-ISOPOOH, the sample evaporated completely and gave a sensitivity of 1.6×10^{-4} ncts/pptv. The (1,2)-ISOPOOH gave a sensitivity of 1.5×10^{-4} ncts/pptv but with a slight residual mass, and 1.6×10^{-4} ncts/pptv was determined appropriate for both isomers.

S2.0 Impurity Oxidation Products The main impurities in the ISOPOOH samples, 2-methyl-1-butene-3,4-diol for (4,3)-ISOPOOH and 3-methyl-1-butene-3,4-diol for (1,2)-ISOPOOH, also react with OH to produce some of the same product masses as ISOPOOH. To correct for the impurity oxidation products, both methylbutanediols were synthesized and each was oxidized by OH under similar conditions to the ISOPOOH experiments. The ratio of the product formation to methylbutanediol loss was then used to remove the methylbutanediol products from the ISOPOOH experiment data.

S3.0 *Ab Initio* Calculations We used the M06-2X/aug-cc-pVTZ method as implemented in the Gaussian 09 program.[3] Frequency calculations were done at all stationary points with the same method to ensure that the equilibrium structures (reactants, reactive complexes, products) only have positive vibrational frequencies and the transition states have one imaginary frequency. To ensure that the transition state connects the reactive complex and the product, intrinsic reaction coordinate (IRC) calculations[4,5] were performed and, if needed, the end product was optimized. None of the M06-2X/aug-cc-pVTZ calculations have any significant spin contamination. Single point energy CCSD(T)-F12a/VDZ-F12 [F12] calculations[6,7] were performed on the M06-2X/aug-cc-pVTZ geometries. All the CCSD(T) calculations were carried out with the Molpro2012 program[8] suite using default convergence criteria. High T1-diagnostic values were observed for H-abstraction from the OH group, and we have therefore used the M06-2X/aug-cc-pVTZ energies for Mesmer modeling. High T1-diagnostic values have been observed previously for H-shift from OH groups.[9,10] For OH addition and H-abstraction involving -CH_2 and >CH groups, the M06-2X/aug-cc-pVTZ energies of the reactant complex and the transition state are in good agreement with the CCSD(T)-F12A/VDZ-F12 energies. The M06-2X/aug-cc-pVTZ (and wb97-XD) method has also previously been found to calculate barrier heights similar to those obtained with the much more computationally expensive CCSD(T)-F12A/VD2-F12 single point calculations on the DFT geometry.[10] In the following we are therefore using the M06-2X/aug-cc-pVTZ energies for kinetic modeling.

S3.1 The energetics of the reaction between ISOPOOH and OH We have assumed that the association reaction between OH and ISOPOOH produces a reactive complex (ISOPOOH-OH). The reactive complex can hereafter overcome the transition state and produce the different product complexes and products.

$$OH + ISOPOOH \rightarrow ISOPOOH\text{-}OH \rightarrow Products$$

In Figures S1 and S2 the different reaction pathways for (1,2)-ISOPOOH and (4,3)-ISOPOOH are shown, respectively, and the energetics of the reaction pathways are given in Tables S1 and S2. The reactant complexes for each of the individual reaction path are different.

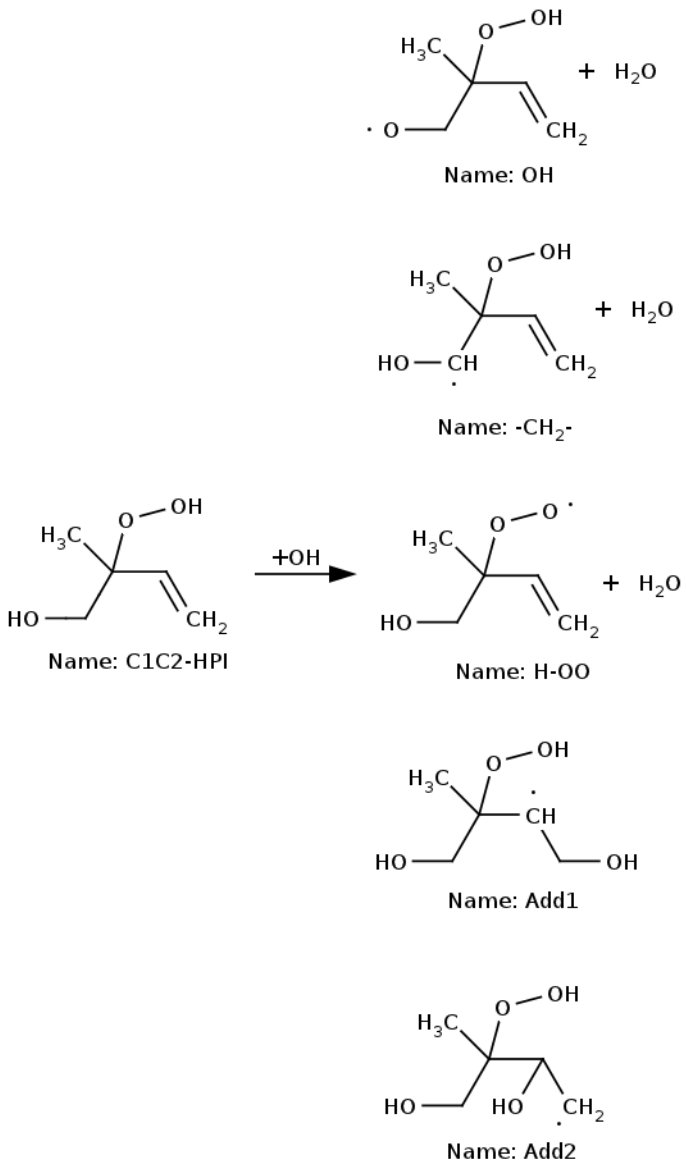

Figure S1. The different reaction pathways for the reaction between (1,2)-ISOPOOH and OH radical.

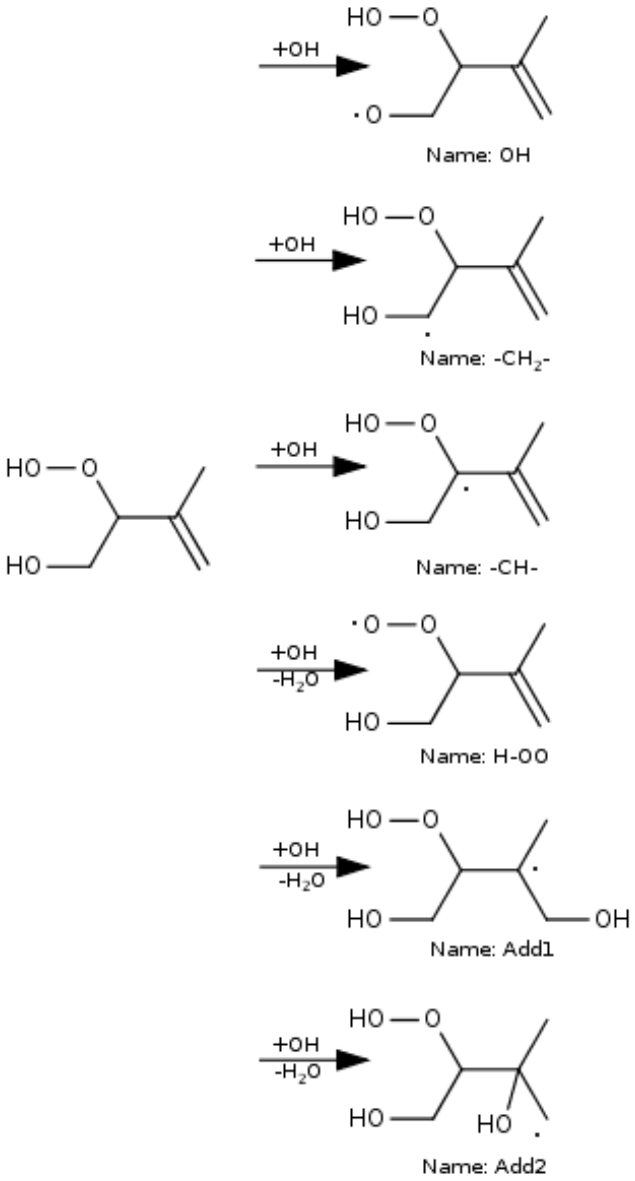

Figure S2. The different reaction pathways for the reaction between (4,3)-ISOPOOH and OH radical.

Table S1. The relative energies (kcal/mol) for the reaction between the (1,2)-ISOPOOH molecule and the OH radical with the M06-2X/aug-cc-pVTZ method and the F12//M06-2X/aug-cc-pVTZ. The values in () are the F12//M06-2X/aug-cc-pVTZ values. The energies are corrected with zero point vibrational energies.

	OH	**-CH_2-**	**H-OO**	**Add1**	**Add2**
(1,2)-ISOPOOH+OH	0.0	0.0	0.0	0.0	0.0
Reactive Complex	-8.9 (-8.3)	-7.3 (-6.1)	-5.0 (-3.7)	-6.2 (-6.1)	-7.8 (-6.2)
Transition State	-2.2 (-1.0[a])	-4.0 (-3.5)	-3.8 (-3.3)	-5.3 (-5.2)	-5.6 (-5.4)
Product Complex	-21.8 (-20.9)	-34.0 (-33.0)	-40.8 (-40.2)	-	-
Product	-13.8 (-8.7)	-24.2 (-23.5)	-34.7 (-34.4)	-34.4 (-31.1)	-33.4 (-30.0)

[a]This calculation has a T1 diagnostic value of 0.078

Table S2. The relative energies (kcal/mol) for the reaction between (4,3)-ISOPOOH and OH with the M06-2X/aug-cc-pVTZ method and the F12//M06-2X/aug-cc-pVTZ. The values in () are the F12//M06-2X/aug-cc-pVTZ values.. The energies are corrected with zero point vibrational energies.

	OH	**-CH_2-**	**-CH-**	**H-OO**	**Add1**	**Add2**
(4,3)-ISOPOOH+OH	0.0	0.0	0.0	0.0	0.0	0.0
Reactive Complex	-6.2 (-5.3)	-6.8 (-6.2)	-6.4 (-4.9)	-5.7 (-4.4)	-7.7 (-6.5)	-5.8 (-4.3)
Transition State	-0.4 (25.6[a])	-1.7 (-1.3)	-4.8 (-4.5)	-2.8 (-1.5[b])	-7.7 (-7.0)	-2.7 (-5.1)
Product Complex	-19.4 (-18.1)	-30.6 (-29.2)	-43.0 (-41.3)	-36.0 (-35.1)	-	-
Product	-10.8 (-9.7)	-23.2 (-22.5)	-33.9 (-34.2)	-33.4 (-33.2)	-34.9 (-31.7)	-31.2 (-28.7)

[a]This calculation has a T1 diagnostic value of 0.116
[b]This calculation has a T1 diagnostic value of 0.058

S3.2 The kinetics of the reaction between ISOPOOH and OH The kinetic calculations are carried out using the master equation solver for multi energy well reaction, MESMER program.[11,12] The general reaction scheme is shown in Figure S3.

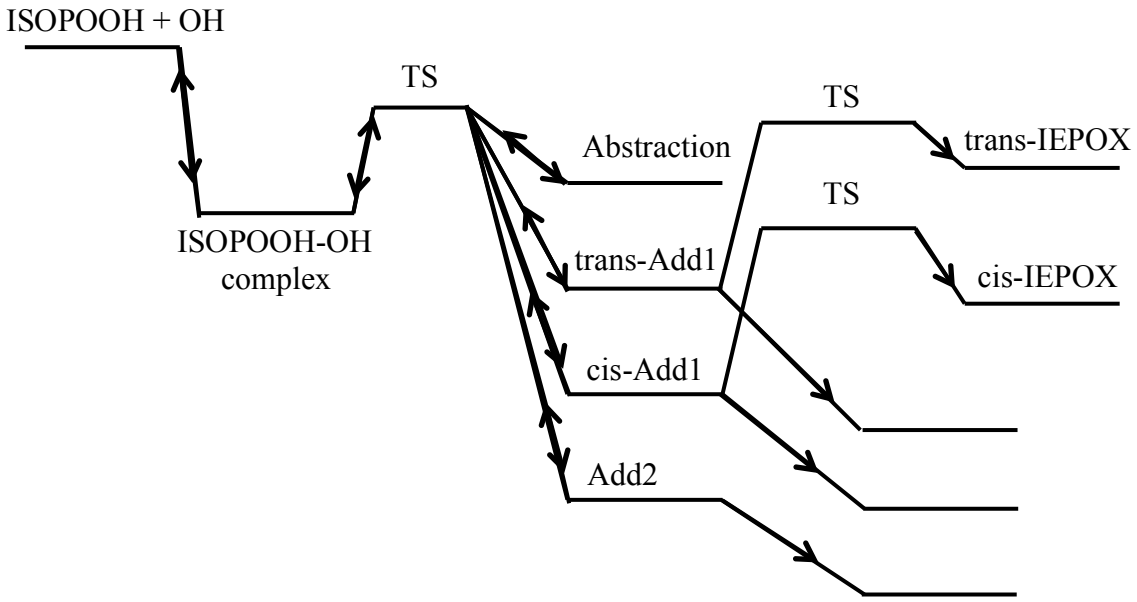

Figure S3. The reaction scheme as used in the MESMER model (Only an illustration, not the energetically correct picture of the reactions). The ISOPOOH-OH complexes are different for each of the reaction pathways even though they are given with the same energy at this figure.

In our Mesmer modeling the Lennard-Jones (L-J) parameters of the bath gas were chosen to be a nitrogen gas resembling the atmospheric gas ($\sigma\,(N_2) = 3.919$ Å, $\varepsilon/k_b\,(N_2) = 91.85$ K) whereas the reactive complex (ISOPOOH-OH) is modeled with the L-J parameters of methylcyclohexane (σ *(methylcyclohexane) = 7.045 Å,* ε/k_b *(methylcyclohexane) = 379.95 K)*.[13] The average collisional activation/deactivation energy transfer of all the molecules is set to 200 cm^{-1} per collision and the grain size of each grain is 50 cm^{-1}. The span of the energy grains is set to 30 *k*T above the highest stationary point. We have used a pressure of 745 Torr and a temperature of 298 K for all the calculations, similar to the experimental conditions.

We have preformed a sensitivity test of Mesmer input parameters. In our sensitivity test we used three collisional activation/deactivation energies of 50, 100 and 200 cm^{-1} and two different grain sizes of 25 and 50 cm^{-1}. We did not observe any significant changes in the reaction rate constants (only changes of a few percent). We have also tested the system with different sizes of grain span, e.g., 10 *k*T, 20 *k*T, 30 *k*T, 40 *k*T and 50 *k*T. If a grain span of 30 *k*T or higher is used, the reaction rate constants do not change. We have therefore used a grain size of 30 *k*T.

The reaction rate constants are sensitive to the choice of the Arrhenius pre-exponential factor (A). Each reaction pathway is a separate Mesmer calculation (See Figure S4 and S5 for the individual reaction pathways) – we have not coupled between the reactions in the fitting of the Arrhenius pre-exponential factor (A). We treat the pre-exponential factor as temperature independent and it is varied between 1.0×10^{-12} and 2.0×10^{-10} cm^3 $molecule^{-1}$ s^{-1}. We use nine different Arrhenius pre-exponential factors to calculate the rates. Three of the factors are from the three reactions of n-butane, 3-methyl-3-butene-1-ol and 1-butene with OH.[14-16] The total reaction rate constants (OH +ISOPOOH → Products) of the (1,2)-ISOPOOH and (4,3)-ISOPOOH systems are shown in Table S3 and Table S4, respectively.

S3.3 (1,2)-ISOPOOH For the (1,2)-ISOPOOH + OH reactions, the absolute rate constants of all the different reaction pathways increase with an increase in the Arrhenius pre-exponential factor, and the relative yields (in %) of the reaction pathways also change. The yield of the two addition reactions increased more compared to yield of the three abstraction reaction pathways with increasing Arrhenius pre-exponential factor. The rate constant is sensitive to the Arrhenius pre-exponential factor since the energy of the transition state is below the energy of the individual reactants. The rate constant for each reaction path is therefore almost identical to the Arrhenius pre-exponential factor.

With an Arrhenius pre-exponential factor of 1×10^{-11} cm^3 $molecule^{-1}$ s^{-1} for the OH abstraction reactions and 6×10^{-11} cm^3 $molecule^{-1}$ s^{-1} for the addition reactions (see Mix

column, Table S3), the yield of the (1,2)-ISOPOOH + OH reactions is OH (1.1), -CH_2- (7.0), H-OO (7.9), Add1 (53.7), and Add2 (30.2). The rate constant for abstraction is 1.2×10^{-11} cm^3 $molecule^{-1}$ s^{-1} and the rate constant for addition is 6.2×10^{-11} cm^3 $molecule^{-1}$ s^{-1}. The sum of the OH addition and OH abstraction rate constants are 7.4×10^{-11} cm^3 $molecule^{-1}$ s^{-1}, and was constrained to mimic the experimentally determined rate.

S3.4 (4,3)-ISOPOOH With an Arrhenius pre-exponential factor of $5x10^{-12}$ cm^3 $molecule^{-1}$ s^{-1} for the OH abstraction reactions and $1.5x10^{-10}$ cm^3 $molecule^{-1}$ s^{-1} for the addition reactions (see Mix column, Table S4), the yield of the (4,3)-ISOPOOH + OH reactions is OH (0.1), -CH_2- (0.5), -CH- (4.0), H-OO (2.3), Add1 (89.0), and Add2 (4.1). The rate constant for abstraction is 7.2×10^{-12} cm^3 $molecule^{-1}$ s^{-1} and the rate constant for addition is 9.7×10^{-11} cm^3 $molecule^{-1}$ s^{-1}. The sum of these, 1.1×10^{-10} cm^3 $molecule^{-1}$ s^{-1}, was constrained to mimic the experimentally determined rate.

Table S3. The reaction rate constants at 298K (in cm^3 $molecules^{-1}$ s^{-1}) for the reaction between the (1,2)-ISOPOOH molecule and the OH radical with the M06-2X/aug-cc-pVTZ method. All the reaction rates are without tunneling correction. In () are the yields in percent. The ratios are calculated as $\Gamma_i=k_i/k_{tot}*100\%$, where $k_{tot} = \Sigma k_i$

Absolute rate (yield, %)	A($1\cdot10^{-12}$)[a]	A($2\cdot10^{-12}$)	A($5\cdot10^{-12}$)[b]	A($1\cdot10^{-11}$)	A($3\cdot10^{-11}$)[c]	A($6\cdot10^{-11}$)	A($1\cdot10^{-10}$)	A($1.5\cdot10^{-10}$)	A($2\cdot10^{-10}$)	**Mix**[d]
OH	*$3.3\cdot10^{-13}$* *(8.3)*	*$4.7\cdot10^{-13}$* *(6.4)*	*$6.8\cdot10^{-13}$* *(4.2)*	*$8.2\cdot10^{-13}$* *(3.0)*	*$1.0\cdot10^{-12}$* *(1.7)*	*$1.1\cdot10^{-12}$* *(1.2)*	*$1.2\cdot10^{-12}$* *(1.0)*	*$1.2\cdot10^{-12}$* *(0.8)*	*$1.2\cdot10^{-12}$* *(0.8)*	***$8.2\cdot10^{-13}$*** ***(1.1)***
$-CH_2-$	*$8.6\cdot10^{-13}$* *(21.8)*	*$1.6\cdot10^{-12}$* *(21.4)*	*$3.2\cdot10^{-12}$* *(20.2)*	*$5.2\cdot10^{-12}$* *(18.7)*	*$9.2\cdot10^{-12}$* *(15.5)*	*$1.2\cdot10^{-11}$* *(13.5)*	*$1.4\cdot10^{-11}$* *(12.1)*	*$1.6\cdot10^{-11}$* *(11.0)*	*$1.7\cdot10^{-11}$* *(10.4)*	***$5.2\cdot10^{-12}$*** ***(7.0)***
H-OO	*$9.0\cdot10^{-13}$* *(22.8)*	*$1.7\cdot10^{-12}$* *(22.8)*	*$3.6\cdot10^{-12}$* *(22.3)*	*$5.8\cdot10^{-12}$* *(21.2)*	*$1.1\cdot10^{-11}$* *(18.3)*	*$1.4\cdot10^{-11}$* *(16.1)*	*$1.7\cdot10^{-11}$* *(14.3)*	*$1.9\cdot10^{-11}$* *(13.2)*	*$2.0\cdot10^{-11}$* *(12.4)*	***$5.8\cdot10^{-12}$*** ***(7.9)***
Add1 (C1)	*$9.8\cdot10^{-13}$* *(24.9)*	*$1.9\cdot10^{-12}$* *(26.3)*	*$4.7\cdot10^{-12}$* *(29.3)*	*$9.0\cdot10^{-12}$* *(32.6)*	*$2.3\cdot10^{-11}$* *(39.4)*	*$4.0\cdot10^{-11}$* *(44.3)*	*$5.6\cdot10^{-11}$* *(48.0)*	*$7.2\cdot10^{-11}$* *(50.6)*	*$8.5\cdot10^{-11}$* *(52.4)*	***$4.0\cdot10^{-11}$*** ***(53.7)***
Add2 (C2)	*$8.8\cdot10^{-13}$* *(22.3)*	*$1.7\cdot10^{-12}$* *(23.0)*	*$3.8\cdot10^{-12}$* *(24.0)*	*$6.8\cdot10^{-12}$* *(24.6)*	*$1.5\cdot10^{-11}$* *(25.1)*	*$2.2\cdot10^{-11}$* *(24.9)*	*$2.9\cdot10^{-11}$* *(24.6)*	*$3.5\cdot10^{-11}$* *(24.3)*	*$3.9\cdot10^{-11}$* *(24.0)*	***$2.2\cdot10^{-11}$*** ***(30.2)***

[a] *Pre-exponential factor from an OH reaction with n-butane (Abstraction) [3].*

[b] *Pre-exponential factor from the reaction of OH with 3-methyl-3-buten-1-ol (Addition and Abstraction)[4].*

[c] *Pre-exponential factor from OH and 1-butene (Addition)[5].*

[d] In the Mix column, the addition and the abstraction reactions use an Arrhenius value of $6\cdot10^{-11}$ and $1\cdot10^{-11}$ cm^3 $molecule^{-1}$ s^{-1}, respectively.

Table S4. The absolute reaction rates at 298K in units of cm^3 $molecules^{-1}$ s^{-1} for the OH radical reaction with the (4,3)-ISOPOOH molecule with the M06-2X/aug-cc-pVTZ method. All the reaction rates are without tunneling correction. In () are the ratios of the different OH and (4,3)-ISOPOOH reactions shown. The ratios are calculated as $\Gamma_i=k_i/k_{tot}*100\%$, where $k_{tot} = \Sigma k_i$

Absolute rate (yield, %)	$A(1\cdot10^{-12})$[a]	$A(2\cdot10^{-12})$	$A(5\cdot10^{-12})$[b]	$A(1\cdot10^{-11})$	$A(3\cdot10^{-11})$[c]	$A(6\cdot10^{-11})$	$A(1\cdot10^{-10})$	$A(1.5\cdot10^{-10})$	$A(2\cdot10^{-10})$	**Mix**[d]
OH	$7.1\cdot10^{-14}$ (1.2)	$7.7\cdot10^{-14}$ (1.2)	$8.1\cdot10^{-14}$ (0.6)	$8.2\cdot10^{-14}$ (0.4)	$8.4\cdot10^{-14}$ (0.2)	$8.5\cdot10^{-14}$ (0.1)	$8.5\cdot10^{-14}$ (0.1)	$8.5\cdot10^{-14}$ (0.1)	$8.5\cdot10^{-14}$ (0.0)	**$8.1\cdot10^{-14}$ (0.1)**
$-CH_2-$	$3.1\cdot10^{-13}$ (6.8)	$4.2\cdot10^{-13}$ (6.8)	$5.5\cdot10^{-13}$ (4.4)	$6.3\cdot10^{-13}$ (3.0)	$7.2\cdot10^{-13}$ (1.6)	$7.7\cdot10^{-13}$ (1.0)	$7.9\cdot10^{-13}$ (0.7)	$8.0\cdot10^{-13}$ (0.6)	$8.1\cdot10^{-13}$ (0.5)	**$5.5\cdot10^{-13}$ (0.5)**
-CH-	$9.3\cdot10^{-13}$ (29.3)	$1.8\cdot10^{-12}$ (29.3)	$4.1\cdot10^{-12}$ (33.3)	$7.4\cdot10^{-12}$ (35.7)	$1.7\cdot10^{-11}$ (36.3)	$2.5\cdot10^{-11}$ (33.6)	$3.2\cdot10^{-11}$ (30.3)	$3.9\cdot10^{-11}$ (27.2)	$4.4\cdot10^{-11}$ (24.9)	**$4.1\cdot10^{-12}$ (4.0)**
H-OO	$7.9\cdot10^{-13}$ (21.8)	$1.3\cdot10^{-12}$ (21.8)	$2.4\cdot10^{-12}$ (19.1)	$3.3\cdot10^{-12}$ (15.9)	$4.8\cdot10^{-12}$ (10.5)	$5.5\cdot10^{-12}$ (7.4)	$6.0\cdot10^{-12}$ (5.6)	$6.3\cdot10^{-12}$ (4.4)	$6.5\cdot10^{-12}$ (3.7)	**$2.4\cdot10^{-12}$ (2.3)**
Add1 (C1)	$6.9\cdot10^{-13}$ (22.3)	$1.4\cdot10^{-12}$ (22.3)	$3.4\cdot10^{-12}$ (27.4)	$6.8\cdot10^{-12}$ (32.7)	$2.0\cdot10^{-11}$ (44.0)	$3.9\cdot10^{-11}$ (52.7)	$6.4\cdot10^{-11}$ (59.4)	$9.2\cdot10^{-11}$ (64.7)	$1.2\cdot10^{-10}$ (68.3)	**$9.2\cdot10^{-11}$ (89.0)**
Add2 (C2)	$7.0\cdot10^{-13}$ (18.5)	$1.1\cdot10^{-12}$ (18.5)	$1.9\cdot10^{-12}$ (15.2)	$2.5\cdot10^{-12}$ (12.1)	$3.4\cdot10^{-12}$ (7.5)	$3.8\cdot10^{-12}$ (5.2)	$4.1\cdot10^{-12}$ (3.8)	$4.3\cdot10^{-12}$ (3.0)	$4.4\cdot10^{-12}$ (2.5)	**$4.3\cdot10^{-12}$ (4.1)**

[a] *Pre-exponential factor from an OH reaction with n-butane (Abstraction) [3]*

[b] *Pre-exponential factor from the reaction of OH with 3-methyl-3-buten-1-ol (Addition and Abstraction)[4].*

[c] *Pre-exponential factor from OH and 1-butene (Addition) [5].*

[d] In the Mix column, the addition and the abstraction reactions use an Arrhenius value of $1.5\cdot10^{-10}$ and $5\cdot10^{-12}$ cm^3 $molecule^{-1}$ s^{-1}, respectively.

S3.5 IEPOX production The formation of *cis*-β-IEPOX (*cis*-C_1C_2), the product of the addition to C_1 in (1,2)-ISOPOOH, has a rate constant (the "energetically cold" reaction rate constant) which is three times faster than the rate constant for the formation of *trans*-β-IEPOX (trans-C_1C_2). The *trans*-β-IEPOX (trans-C_4C_3) rate is faster than the *cis*-β-IEPOX (*cis*-C_4C_3) production rate in the (4,3)-ISOPOOH+OH reaction. The *trans*-C_4C_3 rate constant is fastest because of a lower transition state barrier. The differences between the reaction rate constants of the *cis/trans*-C_1C_2 isomers are due to changes in the vibrational partition functions (Table S5).

We have used the bimolecular reaction rate constant obtained by Park et al.[7], 2.3×10^{-12} cm^3 $molecule^{-1}$ s^{-1} for the reaction between molecular oxygen and OH-isoprene, to represent the bimolecular reaction between our OH addition products and molecular oxygen. With the Park et al. reaction rate constant and a molecular oxygen concentration of 5.2×10^{18} molecule cm^{-3} the pseudo-first order reaction rate becomes 1.2×10^7 s^{-1}.

The "cold" reaction rate constants are estimated using transition state theory including the quantum tunneling given by

$$k_{TST} = \frac{k_B T}{h}\frac{Q_{TS}}{Q_R}\exp\left(-\frac{\Delta E}{k_B T}\right)$$

where Q_R and Q_{TS} are the partition functions for the reactant, R, and the transition state, TS, respectively.[18] The rigid rotor and harmonic oscillator approximations have been used to calculate the partition functions. The energy ΔE is the energy difference between the transition state and the reactant. The constants, h and k_B, are the Planck constant and the Boltzmann constant, respectively. Tunneling was done with the Eckart approach.[19]
The "cold" TST reaction rate constants are all much slower than the estimated pseudo-first order reaction rate constant of the OH-addition ISOPOOH products and molecular oxygen. With this reaction rate constant the bimolecular reaction dominates over the *cis/trans*-β-IEPOX production at atmospheric pressures.

Table S5. The energy barriers, transition state theory (TST) reaction rate constants and the Eckart-corrected TST reaction rate constants for the production of IEPOX. The energies are calculated with the M06-2X/aug-cc-pVTZ method.

Species	ΔE forward / (kcal/mol)	k_{TST} / (s^{-1})	$k_{TST} \cdot \kappa_{Eckart}$ / (s^{-1})
cis-C_1C_2	12.8	3.7×10^{3}	9.2×10^{3}
trans-C_1C_2	12.8	1.1×10^{3}	2.8×10^{3}
cis-C_4C_3	12.4	2.1×10^{3}	4.9×10^{3}
trans-C_4C_3	10.6	3.5×10^{4}	7.4×10^{4}

S3.6 Mesmer Modeling Our MESMER models have all the ISOPOOH+OH reactions along with the *cis/trans*-β-IEPOX production reactions that occur following the OH addition to the outer carbon. All the reactions are shown in Figure S4 and Figure S5 for the (1,2)-ISOPOOH and (4,3)-ISOPOOH molecules, respectively. We have used a grain size of 50 cm^{-1} and a grain span in the model of 30 kT (above the ISOPOOH+OH energy stationary point). We used a collisional activation/deactivation energy of 200 cm^{-1} per bath gas (N_2) collision, a temperature of 298.15 K, a pressure of 745 Torr and an OH concentration of 10^6 molecules cm^{-3}.

(1,2)-ISOPOOH+OH The yields of each component are shown on Figure S4. The total for the compounds' yields shown in bold add to 100%. Our model suggests that only a minor amount of the ISOPOOH-OH molecules are stabilized in the ISOPOOH-OH well.
For the (1,2)-ISOPOOH+OH reaction in Figure S4, we observe that the two addition reactions (Add1 and Add2) dominate over all the OH abstraction reactions. All OH abstraction reactions have yields that are lower than 7%. The OH addition to the inner carbon of the double bond has a yield of 29% of the total yield. After the inner OH addition, molecular oxygen adds and a hydroperoxydiol peroxy radical is produced.

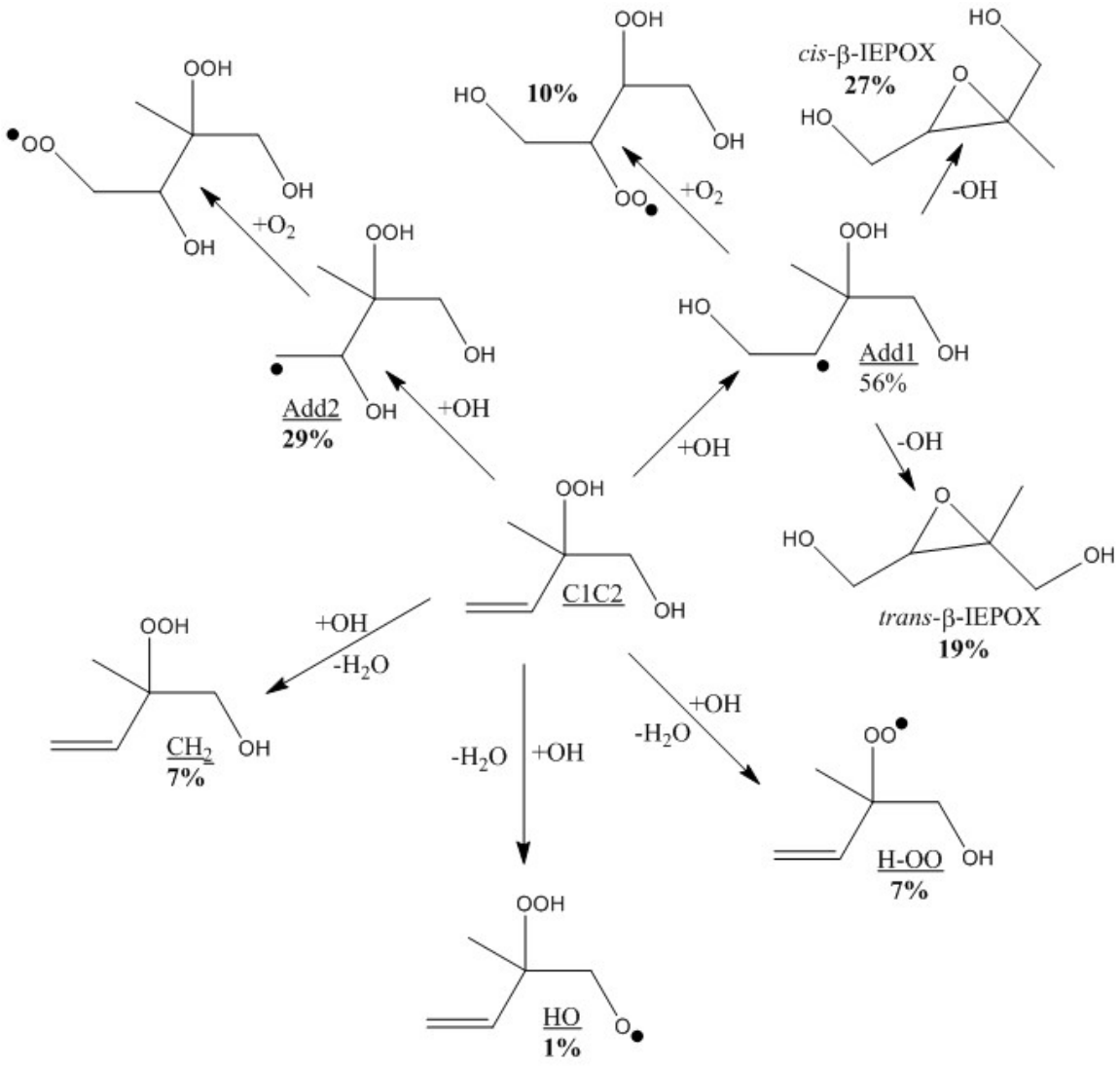

Figure S4. The reactions for the (1,2)-ISOPOOH with OH.

The H-shift between the hydroperoxy hydrogen and the peroxy radical is calculated to be very fast (~10^4 s^{-1}) – much faster than the bimolecular chemistry – so an equilibrium distribution between the two peroxy radicals will result. The calculations suggest that the peroxy radical on C_2 will be favored.

The yield of the OH addition to the outer carbon is 56%. After the OH addition, the molecule can either produce *cis/trans*-β-IEPOX or a peroxy hydroperoxydiol molecule. Our model shows that the excess energy is high enough to overcome the energy barriers and to produce a high yield of β-IEPOX molecules. The 56% of OH addition to the outer carbon will divide into a production of a total yield of 19% *trans*-β-IEPOX, 27% *cis*-β-IEPOX molecule and 10% will add O_2 yielding a hydroperoxydiol peroxy radical. H-shift between the hydroperoxy hydrogen and the peroxy radical is also calculated to be very fast (~10^4 s^{-1}) – much faster than the bimolecular chemistry and so, an equilibrium distribution between the two peroxy radicals will result.

(4,3)-ISOPOOH + OH The calculated yields of each component are shown on the Figure S5. The total for the yields shown in bold add to 100%. OH addition to the outer carbon in the double bond dominates with a yield of 95% of the total yield. The yield of the OH abstraction reaction of the hydrogen α to the hydroperoxy group is around 3%, and all other reactions have production yields around 1% or lower. Of the 95% yield added to the outer carbon around 40% will produce the *cis*-β-IEPOX, 47% produce *trans*-β-IEPOX and around 8% will produce the hydroxyperoxydiol peroxy radical. The yield of *cis/trans*-β-IEPOX is much higher for (4,3)-ISOPOOH+OH compared to (1,2)-ISOPOOH+OH.

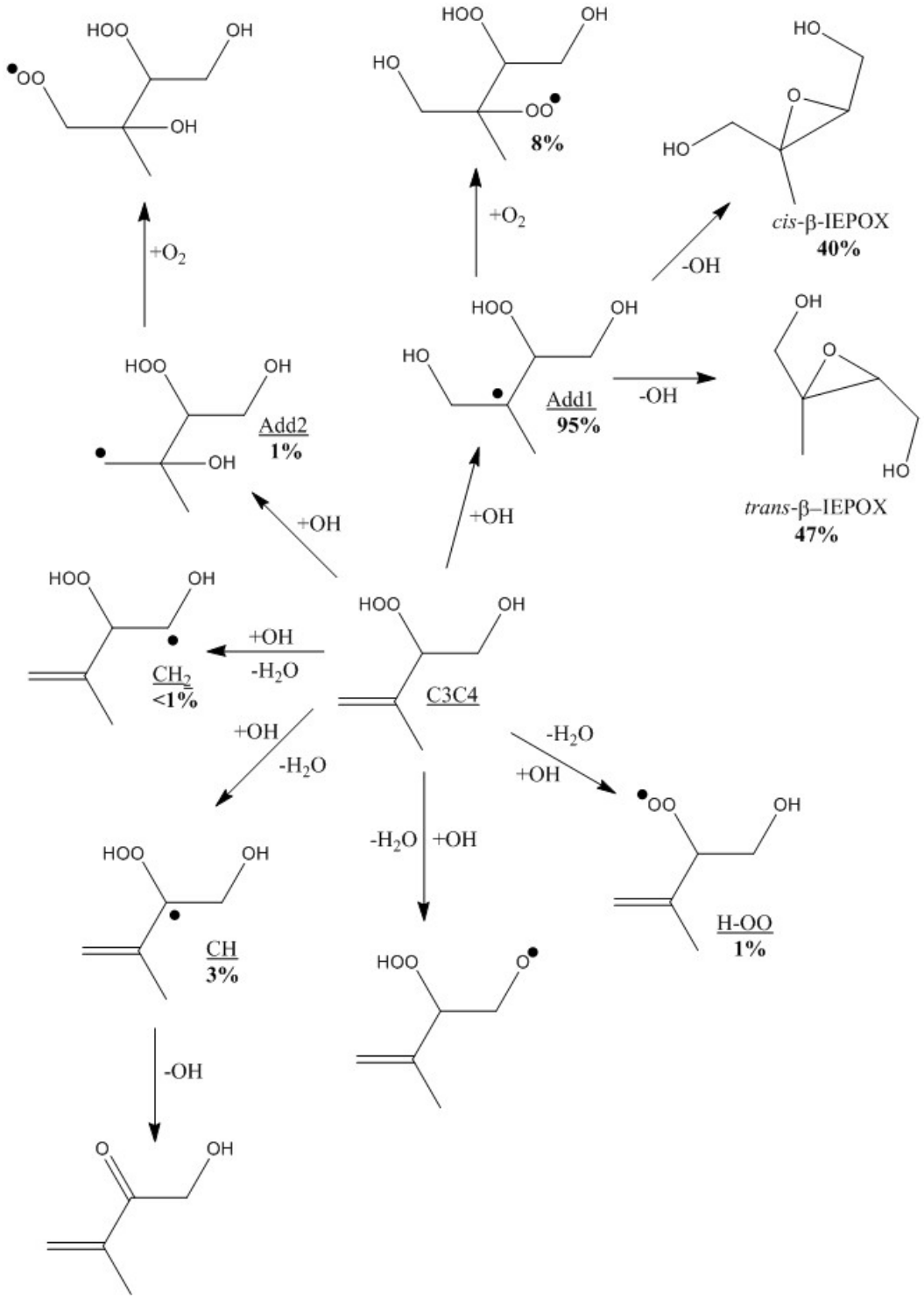

Figure S5. The reactions for the (4,3)-ISOPOOH with OH.

S3.7 Further decomposition after the inner OH addition to the (1,2)-ISOPOOH molecule Following addition of OH to the (1,2)-ISOPOOH via add2, we expect O_2 to add (C4OO) rather than formation of a 4 member epoxide-like compound. After O_2 addition, we find a rapid H-shift from the hydroperoxide group to the ROO (C2OO). A reaction scheme is shown in Figure S6. We have looked at the (R,R)-enantiomer of the molecule and performed preliminary calculations with the `M06-2X/aug-cc-pVTZ` method. The calculated H-shift barrier height for this reaction is found to be 9.3 kcal/mol. The product is 0.4 kcal/mol lower than the reactant. The attachment of molecular oxygen releases an energy of 34.4 kcal/mol compared to the (1,2)-ISOPOOH-OH added product (inner addition), and the energy difference between the (1,2)-ISOPOOH+OH+O_2 and the molecule with the oxygen attached (reactant) is 63.8 kcal/mol. The "cold" TST reaction rate constants, including the Eckart tunneling correction, are 5.6×10^{6} s^{-1} and 5.8×10^{6} s^{-1} for the forward and backward H-shift reactions, respectively.

The second H-shift reaction would likely take the terminal hydrogen with the OOH group, and lead to loss of OH. It has a barrier height of 23.1 kcal/mol and a TST Eckart-corrected reaction rate constant of 1.2×10^{-4} s^{-1}. The energy of the final aldehyde+OH is almost 50.4 kcal/mol lower in energy than the transition state. The energetics are shown in Table S6.

Table S6. The energetics (in kcal/mol) of the two H-shift reactions after the inner OH addition (+O_2) to the (1,2)-ISOPOOH molecule calculated with the M06-2X/aug-cc-pVTZ method.

Species	ΔE+ZPVE / kcal/mol
(1,2)-ISOPOOH+OH+O_2	0.0
C4OO	-63.8
TS	-53.0
C2OO	-64.2
TS	-41.1
Aldehyde+OH	-91.5

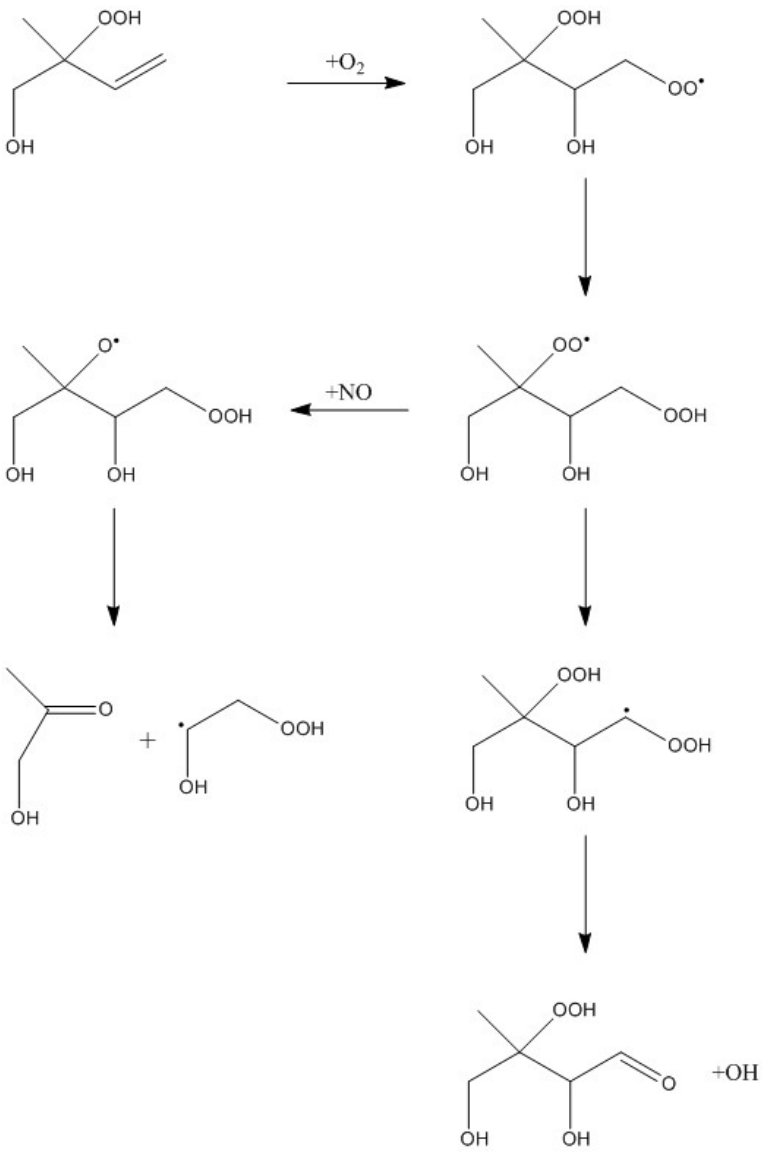

Figure S6. The two possible H-shift reactions after the internal OH addition ($+O_2$) in the (1,2)-ISOPOOH molecule.

S4.0 GEOS-CHEM Calculations

The chemical mechanisms for the 'Standard' and 'Old' GEOS-Chem runs were identical except for the differences included in Table S7. The complete 'Standard' mechanism can be obtained at http://wiki.seas.harvard.edu/geos-chem/index.php/New_isoprene_scheme.

Table S7. Differences between the 'Standard' and 'Old' GEOS-Chem mechanisms.

	'Standard'	'Old'
HO_2+RO_2 rate coefficient	2.91×10^{-13} × exp(1300/T) × [1-exp(-0.245 × n]	7.4×10^{-13} × exp(700/T)
H-abstraction rate coefficient	4.75×10^{-12} × exp(200/T)	3.8×10^{-12} × exp(200/T)
H-abstraction yields	0.387 ISOPOO + 0.613 OH + 0.613 HC5	0.70 ISOPOO + 0.300 HC5 + 0.300 OH

The 'Recommended' simulation run in GEOS-Chem included an increased ISOPOOH yield of 94% from the reaction of HO_2 with ISOPOO, as well as individually speciated ISOPOOH and IEPOX isomers. Listed below are the rates and products of individual reactions edited and added to the GEOS-Chem mechanism in the 'Recommended' simulation to account for the isomers of ISOPOOH and IEPOX. In the GEOS-Chem mechanism, ISOPOOH is referred to as RIP; RIPA, RIPB, and RIPD refer to (1,2), (4,3), and delta (1,4 and 4,1) ISOPOOH respectively, while IEPOXA, IEPOXB, and IEPOXD refer to *trans*-β, *cis*-β, and delta IEPOX respectively. Temperature dependencies of rate constants were kept from the 'standard' GEOS-Chem mechanism.

RIO2 + HO2 → 0.628 RIPA + 0.272 RIPB + 0.037 RIPD + 0.063 (OH + CH2O + HO2) + 0.038 MVK + 0.025 MACR; k = 2.06e-13*exp(1300/T)

RIPA + OH → 0.750 RIO2 + 0.250 HC5 + 0.125 (OH + H2O); k = 6.13e-12*exp(200/T)

RIPA + OH → 0.850 OH + 0.578 IEPOXA + 0.272 IEPOXB + 0.150 HC5OO; k = 1.70e-11*exp(390/T)

RIPB + OH → 0.480 RIO2 + 0.520 HC5 + 0.26 (OH + H2O); k = 4.14e-12*exp(200/T)

RIPB + OH → 1.000 OH + 0.680 IEPOXA + 0.320 IEPOXB; k = 2.97e-11*exp(390/T)

RIPD + OH → 0.250 RIO2 + 0.750 HC5 + 0.375 (OH + H2O); k = 5.11e-12*exp(200/T)

RIPD + OH → 0.500 OH + 0.500 IEPOXD + 0.500 HC5OO; k = 2.92e-11*exp(390/T)

IEPOXA + OH → IEPOXOO; k = 3.73e-11*exp(-400/T)

IEPOXB + OH → IEPOXOO; k = 5.79e-11*exp(-400/T)

IEPOXD + OH → IEPOXOO; k = 3.20e-11*exp(-400/T)

Other reactions involving RIP and IEPOX in the original GEOS-Chem mechanism, including deposition and photolysis, were simply updated to apply to each individual isomer of the two compounds.

References:

1. St. Clair, J. M.; Spencer, K. M.; Beaver M. R.; Crounse, J. D.; Paulot, F.; Wennberg, P. O., Quantification of Hydroxyacetone and Glycolaldehyde Using Chemical Ionization Mass Spectrometry. *Atmos. Chem. Phys*. **2014**, 14, 4251-4262.
2. Liu, Y. J.; Herdlinger-Blatt, I.; McKinney, K. A.; Martin, S. T., Production of Methyl Vinyl Ketone and Methacrolein via the Hydroperoxyl Pathway of Isoprene Oxidation. *Atmos. Chem. Phys.* **2013,** *13* (11), 5715-5730.
3. Frisch, M.; Trucks, G.; Schlegel, H. B.; Scuseria, G.; Robb, M.; Cheeseman, J.; Scalmani, G.; Barone, V.; Mennucci, B.; Petersson, G., Gaussian 09, Revision B.01, Gaussian. *Inc., Wallingford, CT,* **2009**.
4. Gonzalez, C.; Schlegel, H. B., An Improved Algorithm for Reaction-path Following. *J. Chem. Phys.* **1989,** *90*, 2154-2161.
5. Gonzalez, C.; Schlegel, H. B., Reaction-path Following in Mass-weighted Internal Coordinates. *J. Phys. Chem.* **1990,** *94*, 5523-5527.
6. Adler, T. B.; Knizia, G.; Werner, H.-J., A Simple and Efficient CCSD(T)-F12 Approximation. *J. Chem. Phys.* **2007,** *127*, 221106.
7. Peterson, K. A.; Adler, T. B.; Werner, H.-J., Systematically Convergent Basis Sets for Explicitly Correlated Wavefunctions: The Atoms H, He, B-Ne, and Al-Ar. *J. Chem. Phys.* **2008,** *128*, 084102.

8. Werner, H.-J.; Knowles, P. J.; Knizia, G.; Manby, F. R.; Schütz, M.; Celani, P.; Korona, T.; Lindh, R.; Mitrushenkov, A.; Rauhut, G.; et al., *MOLPRO, Version 2012.1, A Package of Ab Initio Programs*, **2012**.
9. Peeters, J.; Nguyen, T. L., Unusually Fast 1,6-H Shifts of Enolic Hydrogens in Peroxy Radicals: Formation of the First-Generation C-2 and C-3 Carbonyls in the Oxidation of Isoprene. *J. Phys. Chem. A* **2012,** *116*, 6134-6141.
10. Knap, H. C.; Jørgensen, S.; Kjaergaard, H. G., Theoretical Investigation of the Hydrogen Shift Reactions in Peroxy Radicals Derived from the Atmospheric Decomposition of 3-methyl-3-buten-1-ol (MBO331). *Chem. Phys. Lett.* **2015,** *619*, 236-240.
11. Robertson, S.H.; Glowacki; D. R., Liang;C.-H., Morley, C.; Shannon, R.; Blitz, M. Seakins, P. W.; Pilling, M. J.; MESMER (Master Equation Solver for Multi-Energy Well Reactions), 2008-2013, an Object Oriented C++ Program Implementing Master Equation Methods for Gas Phase Reactions with Arbitrary Wells. http://sourceforge.net/projects/mesmer.
12. Glowacki, D. R.; Liang, C.-H.; Morley, C.; Pilling, M. J.; Robertson, S. H., MESMER: an Open-source Master Equation Solver for Multi-energy Well Reactions. *J. Phys. Chem. A* **2012,** *116*, 9545-9560.
13. Cuadros, F.; CachaDiña, I.; Ahumada, W., Determination of Lennard-Jones Interaction Parameters Using a New Procedure, *Molecular Engineering* **2013**, *6*, 319-325.
14. Atkinson, R.; Kinetics of Gas-phase Reactions of OH Radicals with Alkanes and Cycloalkanes, *Atmos. Chem. Phys.* **2003**, *3*, 2233-2307.
15. Cometto. P. M.; Dalmasso, P. R.;Taccone, R. A.; Lane, S. I.; Oussar, F.; Daële, V.; Mellouki, A.; Le Bras, G., Rate Coefficients for the Reaction of OH with a Series of Unsaturated Alcohols between 263 and 371 K, *J. Phys. Chem. A* **2008**, *112*, 4444-4450.
16. Vakhtin, A. B.; Murphy, J. E.; Leone, S. R., Low-Temperature Kinetics of Reactions of OH Radical with Ethane, Propene and 1-Butene, *J. Phys. Chem. A* **2003**, *107*, 10055-10062.
17. Park, J.; Jongsma, C. G.; Zhang, R. Y.; North, S. W., OH/OD Initiated Oxidation of Isoprene in the Presence of O2 and NO. *J. Phys. Chem. A* **2004**, *108*, 10688-10697.
18. Henriksen, N. E.; Hansen, F. Y., *Theories of Molecular Reaction Dynamics: The Microscopic Foundation of Chemical Kinetics*. Oxford University Press: New York, **2008**.
19. Eckart, C., The penetration of a potential barrier by electrons. *Phys. Rev.* **1930,** *35*, 1303-1309.